Modeling composition of Ca-Fe-Mg carbonates in a natural CO_2 reservoir

G. BICOCCHI[1], G. MONTEGROSSI[2], G. RUGGIERI[2], A. BUCCIANTI[1,2] & O. VASELLI[1,2]

1) Dept. Earth Sciences, University of Florence, Via La Pira 4, 50121 Florence, ITALY, gabriele.bicocchi@unifi.it
2) CNR - Institute of Geosciences and Earth Resources, Via La Pira 4, 50121 Florence, ITALY

Abstract

Understanding the physical-chemical features of liquid, gas and solid phases in natural analogue reservoirs of Carbon Capture and Sequestration (CCS) site is fundamental as they can provide key data for building up both conceptual and numerical modeling of reaction path for gas-water-rock interaction in high pCO_2 systems. The aim of this work is improve the knowledge about these processes, by employing appropriate methods for compositional data on a case study, focusing on the solid (minerals) phases.

In the early eighties, the PSS1 well (Eastern Tuscany, Central Italy), drilled down to almost 5,000 m for oil exploration by ENI (Italian National Agency of Hydrocarbons), intercepted a high pressure (≈700 bar) CO_2 reservoir at the temperature of 120 °C. The reservoir rocks in the fertile horizon, located at about 3,800 m, consist of altered volcanic deposits interbedded with gypsum-dolomite-bearing evaporites ("Burano Formation"). Surveys for determining the actual paragenesis of volcanic rocks, carried out on the drill core samples, corresponded to the top of CO_2 reservoir (3,864-3,871 m depths from surface on the PSS1 bore-well log). Quartz, Ca-Fe-Mg carbonates, clay minerals (illite and chlorite series) and Fe-Ti oxides were found as principal mineralogical phases. Electron Microprobe Analysis on the carbonates has allowed to recognize the presence of ankerite and calcites.

Compositional data, related to atomic % content of Ca, Fe, and Mg in carbonates minerals, were transformed by using *Isometric Log-Ratio balances*, whilst the variability affecting the data pattern was investigated in simple binary diagrams. The stoichiometric substitution processes governing the presence of Ca, Fe and Mg in carbonates were modeled by using regression techniques in the new space defined by *ilrs* coordinates. Results have evidenced the different role of Fe and Mg in substituting or not Ca in both carbonate minerals of these CO_2-bearing reservoir rocks.

Key words: carbon sequestration, carbonates minerals, composition, isometric log-ratio.

1. PSS1 bore-well

1.1 Geological settings and reservoir characteristics

The PSS1 well is located in the San Cassiano Basin, Tiber Valley (Eastern Tuscany, Central Italy) in an axial zone of the Apenninic Chain; a schematic stratigraphic column, reconstructed (Anelli et al., 1994; Bonini, 2009) by the original ENI well log of 1984, is reported in Figure 1. This portion of the Apennines is part of the foredeep-thrust belt system migrating eastwards and consists of thick turbiditic successions piled-up during the Miocene paroxistic phase. From East to West the following geological units are recognized: the Tuscan (Cervarola-Falterona Formation) and the Romagnolo-Marchigiano (Marnoso-Romagnolo and Monte Nerone Unit) Complexes, which are overlaid by the Liguride Complex and Quaternary deposits.

The subsurface stratigraphic sequence encountered by the PSS1 well can schematically be summarized from the top to the bottom (after Anelli et al., 1994), as follows: Neogene and Liguride Nappes overlaying the Cervarola-Falterona Sandstone Formation, although at the depth of 1,853 m a tectonic discontinuity separates the Cervarola-Falterona Unit from a Paleogene-Mesozoic

sequence. Lower Mesozoic formations (marls and limestones) are found down to 3,500 m followed by the Triassic Burano Formation (mainly consisting of evaporitic deposits). The latter is interbedded with altered calc-alkaline andesitic (?) volcanic products whose K-Ar radiometric age, according to ENI (1984), is to be referred to Oligocene-Miocene (?).

As far as the deep fluid is concerned, a relevant fraction of carbon dioxide is found at a depth of 3,800 m, presumably at the top of the main fluid reservoir, at P-T conditions of nearly 700 bar (70 MPa) and 120 °C, respectively, with a density of 860 kg/m^3, univocally suggesting the presence of a supercritical fluid (Heinicke et al., 2006) at this depth. The main fluid reservoir apparently resides into volcanic rocks with Burano Formation acting as a sealing barrier to the fluids generated into the deeper levels. The chemical composition of the trapped fluid was CO_2 (92.2%), N_2 (7.6%), CH_4 (0.03%), O_2 (0.01%), H_2S (<0.02%) and H_2O (<0.5%) (Heinicke et al., 2006).

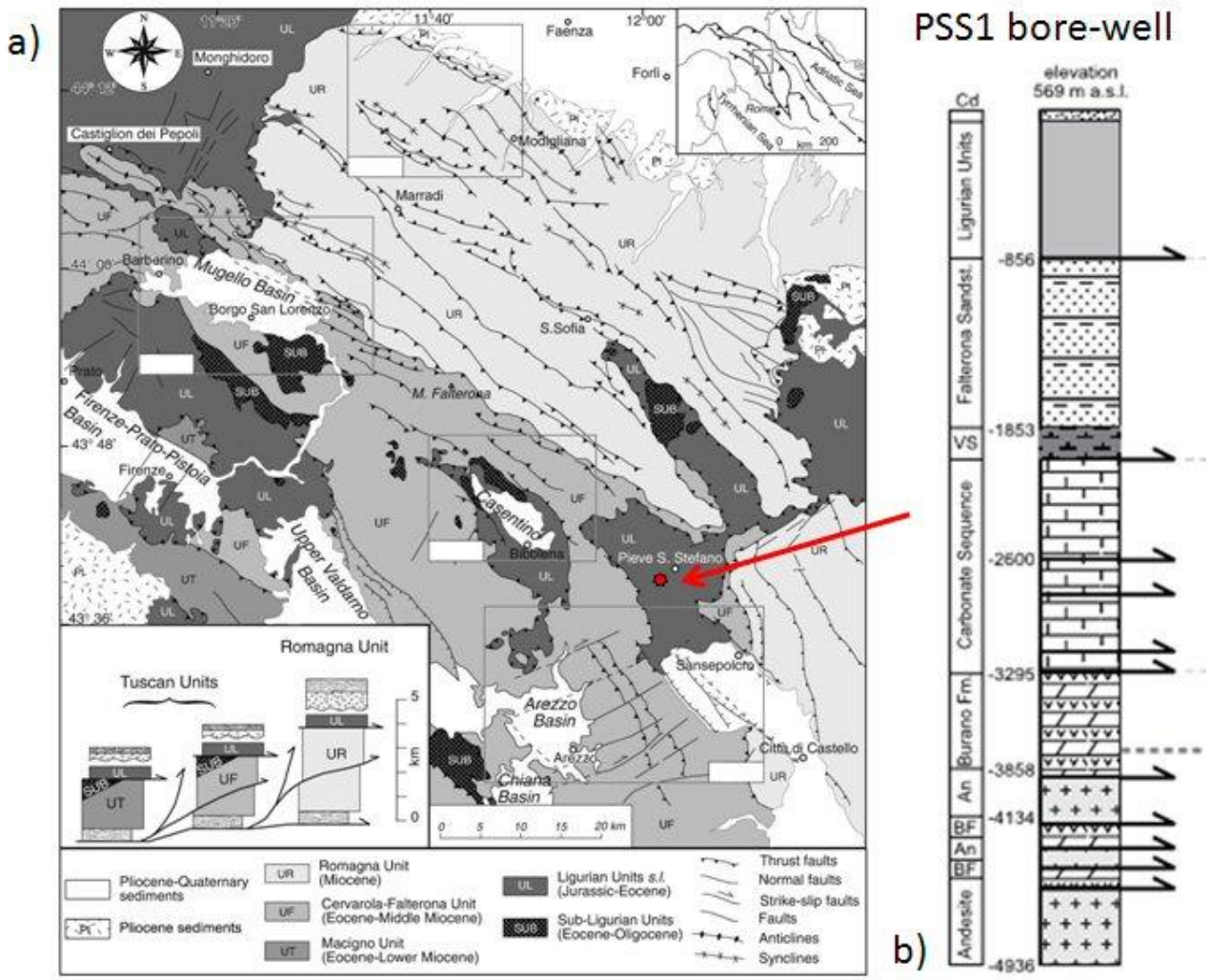

Figure 1. a) Geographical and geological settings of PSS1 in Tiber Valley (modified after Sani et al., 2009); b) reconstruction of stratigraphic column from well log (modified after Bonini, 2009). **Cd** = San Cassiano Pleistocene Continental Deposits, **VS** = Varicoloured Shale, **An** = Andesite, **BF** = Burano Formation.

1.2 Petrographic and mineralogical insight from CO_2 host rocks

According to the description of the cuttings by ENI (1984) the original volcanic rocks of the reservoir top are "andesitic" in composition, on the basis of Total Alkali and Silica diagram (TAS) by Le Bas et al. (1986), reported in Figure 2. Nevertheless, the presence of such CO_2–rich fluid (supported by the high pCO_2 still present in the system) has nearly completely obliterated the

original paragenesis.

The mineralogical assemblage, as derived by drill cores (8 different samples from depth 3,864 to 3,871 m with respect to the well log) investigated nowadays, is indeed consisting of quartz, Ca-Fe-Mg carbonates (mainly calcite and ankerite), clay minerals (illite and chlorite series) and Fe-Ti oxides, all these minerals typically characterized by rather small grain size (from 100 to less than 10 micron). Moreover, quartz, the most abundant silicate mineral observed in the drill cores, appears to have mostly precipitated from an aqueous fluid in a secondary, hydrothermal stage. This process has affected the original composition of the volcanic rocks by likely increasing the original silica content. As a consequence, the classification of the PSS1 volcanic rocks (Figure 2) as andesites has to be likely considered misleading and not realistic. Moreover, it is important to remember that this diagram does not represent an adequate geometry to discriminate samples (e.g. Martin-Fernández et al., 2005).

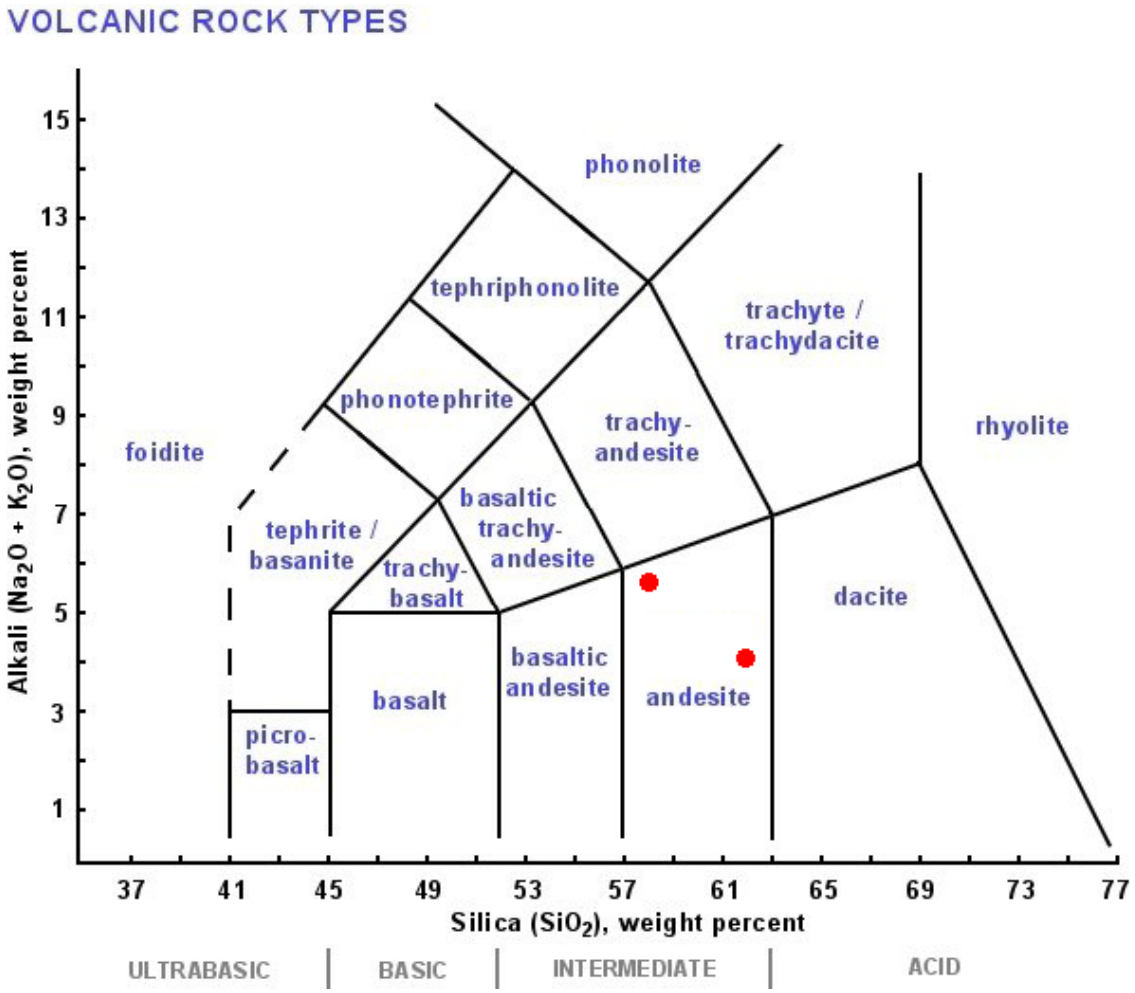

Figure 2. The TAS (Total Alkali vs. Silica) diagram (Le Bas et al., 1986); red dot are two sample of bulk rock from depth 3,870 m of the drill core PSS1 analysed by ENI in 1984.

2. The case study: carbonates minerals composition

2.1 Analytical methods

In this work, polished thin sections from samples from the top of the CO_2 reservoir in volcanic rocks (subsection 1.2) from the PSS1 bore-well, were analysed by SEM-EDS (Scanning Electron Microscope-Electron Dispersive Spectroscopy) at the University of Florence (Department of Earth Sciences) and by EMP (Electronic MicroProbe) at the CNR-IGG (Italian National Council for Research - Institute of Geosciences and Earth Resources) of Padua.

EMP analyses were performed on carbonates for Ca, Fe, Mg, Mn, Sr, Si, O content, with an analytical relative error ranging from 3% (Ca, Fe, Mg, Si, O) to 5% (Sr, Mn). Analyses were controlled for quality with respect to the theoretical stoichiometric ratio of minerals formula. The sum of the cations and anions (CO_3^{2-} groups) was checked to be clustering around 100%, with tolerance set into ± 3 % interval (i.e. excess or defect of cations with respect to anions). Chemical analyses not respecting these criteria were discarded. Back-scattered (BS) imaging was used for better distinguishing the different mineral phases as shown in Figure 3 where a BS photo of quartz and ankerite is reported along with their respective spectra.

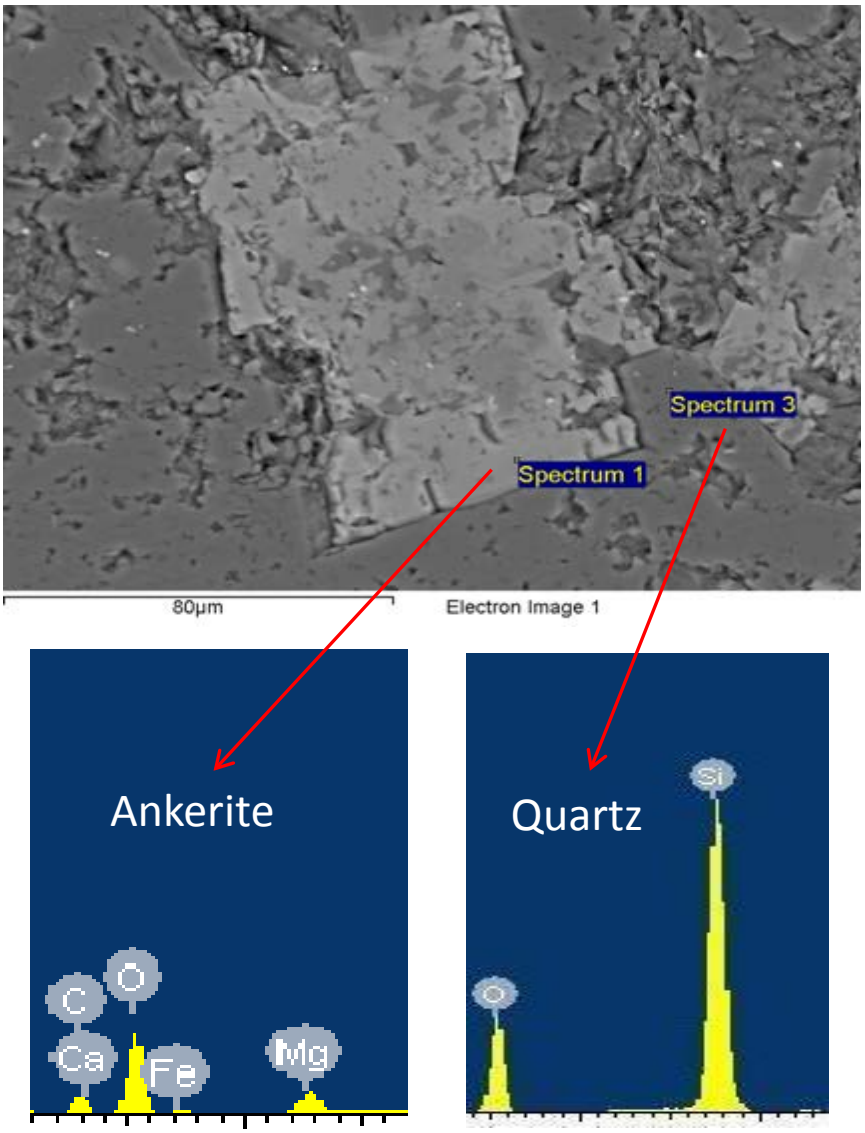

Figure 3. SEM-EDS back-scattered (BS) photo (top) and spectra of ankerite (on the left, lighter minerals on BS photo) and quartz (on the right, darker minerals in the BS photo).

2.2 Carbonates: calcite and dolomite groups

Carbonates are somehow unique minerals as they are one of the few mineral groups able to give information about chemical, physical and biological processes across a wide range of environment (sea, land, fresh water) and throughout much part of the geological time (Reeder, 1983). Carbonates of divalent ions (e.g. Ca^{2+}, Mg^{2+}, Fe^{2+}, Mn^{2+}, Sr^{2+}) are widely present in sedimentary rocks as primary minerals or, generally at minor extent, in metamorphic and magmatic rocks as secondary (neogenetic) minerals; the only exception for magmatic rocks are carbonatites, where carbonates minerals are more than 50% of the bulk composition.

The most common mineral is calcite [$CaCO_3$], which also gives the name to the group of rhombohedral carbonates with calcite-structure. Carbonates are often solid solution of various end-members of calcite-structure as siderite [$FeCO_3$], magnesite [$MgCO_3$], and rodocrosite [$MnCO_3$]. Dolomite [$CaMg(CO_3)_2$] is the end-member of another structure group of carbonates widely present in nature. This group is characterized by two sites for divalent cations in the structure; some dolomite-structure carbonates are ferroan dolomite (dolomite with up to 20% of Fe^{2+} substituting Mg^{2+}), ankerite [$Ca(Fe,Mg)(CO_3)_2$] and kutnahorite [$CaMn(CO_3)_2$]. In the crystalline lattices of calcite and dolomite groups, Fe^{2+} and Mg^{2+} are able to substitute Ca^{2+} (also substitution between Fe^{2+} and Mg^{2+} themselves are possible) in the site for divalent cations (Reeder, 1983).

Because they are mainly present in sedimentary rocks, carbonates are applied to low temperature studies. On the contrary, in our case study, carbonates minerals are not related to sedimentary processes but are likely part of fluid-rock interaction processes at temperature > 100 °C, as deduced from: i) present temperature at depth of the PSS1 (120 °C) and ii) data obtained through the study of some H_2O-rich fluid inclusions in quartz and calcite (still in progress). As carbonates in this environment are likely to be precipitated as secondary minerals after the reaction between rocks and fluids (Montegrossi et al., 2010), their composition would reflect the reaction path between H_2O- and/or CO_2-rich fluids, as also supported by the physical-chemical features of the fluid inclusions.

3. Compositional data processing and modeling

3.1 The choice of the subcomposition

Ternary diagrams are frequently used in Earth Sciences and in particular in Geochemistry, for resuming and inspecting, in geological samples, the abundance of 3 selected components (or end-members) in a bidimensional space. Typical examples are the triangular diagrams of nitrogenated species (NH_4^+-NO_2^--NO_3^-) in waters, the inert gases (N_2-Ar-He) in volcanic gases (e.g. Giggenbach, 1996) and the granulometric fractions in sedimentary rocks and soils (sand-silt-clay).

Data represented in ternary diagrams lie in a constrained space, created in a D-1 space for D components, by forcing them to sum at a constant value *k* (1, 100%, 1 mole...). In this kind of space, commonly known as "simplex" (Aitchinson, 1986), tracing linear paths for describing the data structure and attributing consequentially linear processes to these paths is not theoretically correct, thus leading to erroneous data interpretation. By using proper methods for compositional data (e.g. Buccianti et al., 2006) these problems can be avoided; as a consequence classical statistical tools developed for unconstrained space can be applied. This approach was used for the analysis of compositional data structure, pertaining to the Ca-Fe-Mg subcomposition, with binary diagrams obtained through conversion of coordinates (subsection 3.2), instead of classical ternary diagram (Figure 4).

The compositional data we refer to are, for ankerites, from the depths 3,864 and 3,868 to 3,871 m (66 mineral chemistry analyses), whereas those for calcites range from 3,864 to 3,867 m (80 analyses) (Table 1). In addition of data exposed, composition of an ankerite and a ferroan dolomite retrieved by http://webmineral.com/data were put into the diagrams for comparison.

depths (m) of the bore-well log	*ankerites*	*calcites*
3,864	13	12
3,865	n.a.	21
3,866	n.a.	28
3,867	n.a.	19
3,868	13	n.a.
3,869	15	n.a.
3,870	13	n.a.
3,871	12	n.a.
Total	66	80

Table 1. Summary of the EMP analyses of calcite and ankerite from the PSS1 drill-cores; n.a. = not analysed.

Abundances of Ca, Fe and Mg in calcite and ankerite were expressed in atomic % instead of mol% or wt% in oxides as in other works on stoichiometry for compositional data (e.g. Grunsky et al., 2008). Stoichiometric substitution processes are indeed controlling the presence of these elements in cations sites, whose presence is on the other hand depending on the mineral structure. For focusing on these kind of processes, concentrations with respect to the atoms is, in our opinion, the best unit of measure.

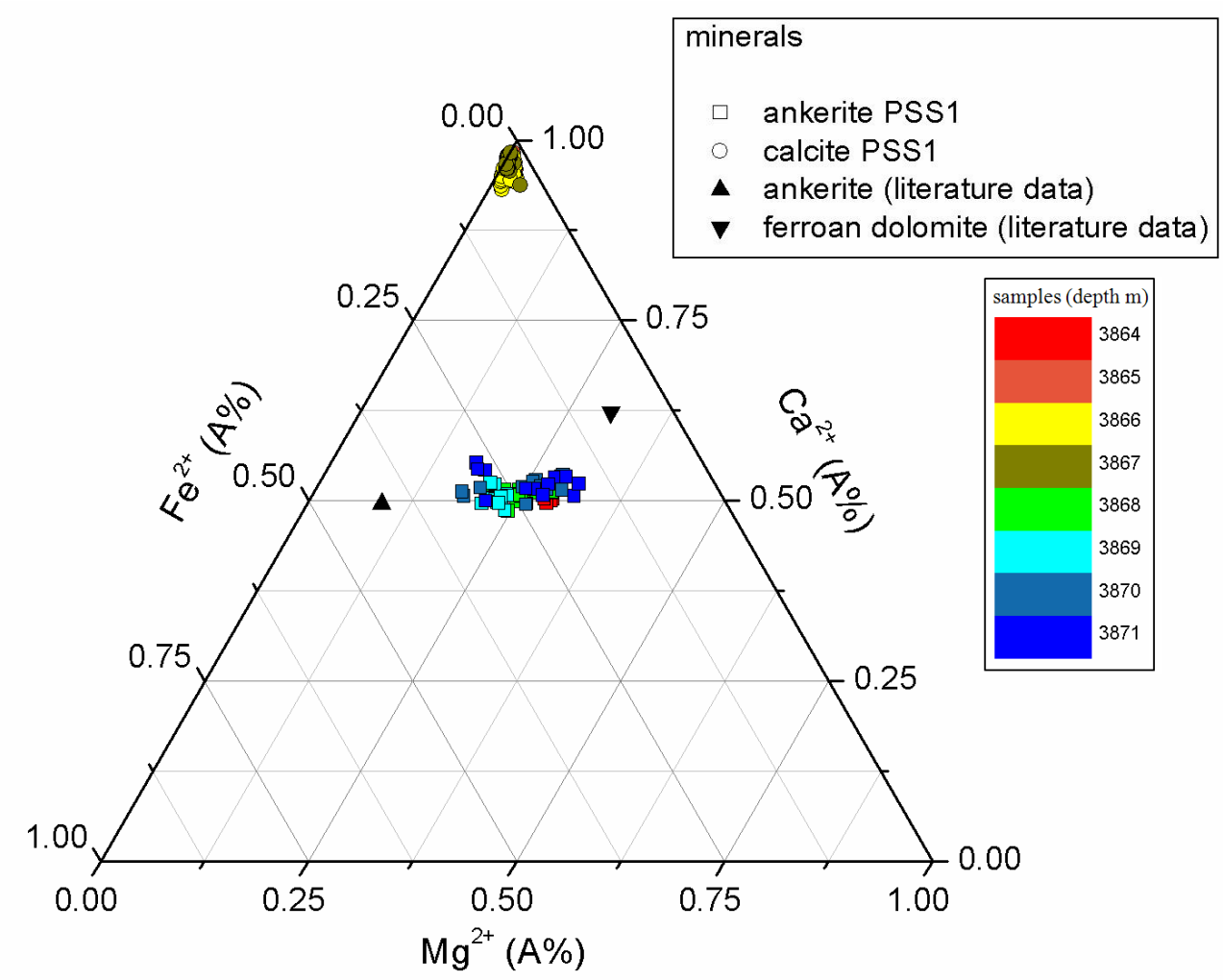

Figure 4. The ternary diagrams of atomic % content of Ca, Fe and Mg for calcite and ankerite from the PSS1 drill cores. For comparison ankerite s.s. (a typical ankerite from literature) and ferroan dolomite from http://webmineral.com/data are also included.

3.2 Exploratory analysis and regression in the *ilr* space

The first step of data processing was the transformations from the original data (content in atomic % of Ca, Fe, and Mg in the carbonates) in isometric-logratio balances (Egozcue et al., 2003). As all the possible couples of variable were to be investigated, we decided to perform the three different possible transformations with respect to the three variables considered in the present study. As a consequence, three systems with a couple of balances were obtained, as follows:

- [3.2.1] $ilr1 = \frac{1}{\sqrt{2}} \cdot ln \frac{Ca}{Fe}$; $ilr2 = \frac{1}{\sqrt{6}} \cdot ln \frac{Ca \cdot Fe}{Mg^2}$.
- [3.2.2] $ilr1 = \frac{1}{\sqrt{2}} \cdot ln \frac{Fe}{Mg}$; $ilr2 = \frac{1}{\sqrt{6}} \cdot ln \frac{Fe \cdot Mg}{Ca^2}$.
- [3.2.3] $ilr1 = \frac{1}{\sqrt{2}} \cdot ln \frac{Ca}{Mg}$; $ilr2 = \frac{1}{\sqrt{6}} \cdot ln \frac{Ca \cdot Mg}{Fe^2}$.

The data structure was then investigated in three new binary diagrams with orthonormal basis. Initially, the variance-covariance matrix and the Pearson correlation index *r* (Table 2), between each couple of *ilrs* balances, which were divided for the two minerals species (ankerites and calcites), were calculated.

ankerites

r = -0.88	*ilr1*	*ilr2*
$ilr1 = \frac{1}{\sqrt{2}} \cdot ln \frac{Ca}{Fe}$	0.013	-0.018
$ilr2 = \frac{1}{\sqrt{6}} \cdot ln \frac{Ca \cdot Fe}{Mg^2}$	-0.018	0.030

r = 0.16	*ilr1*	*ilr2*
$ilr1 = \frac{1}{\sqrt{2}} \cdot ln \frac{Fe}{Mg}$	0.041	0.001
$ilr2 = \frac{1}{\sqrt{6}} \cdot ln \frac{Fe \cdot Mg}{Ca^2}$	0.001	0.002

r = -0.86	*ilr1*	*ilr2*
$ilr1 = \frac{1}{\sqrt{2}} \cdot ln \frac{Ca}{Mg}$	0.011	-0.016
$ilr2 = \frac{1}{\sqrt{6}} \cdot ln \frac{Ca \cdot Mg}{Fe^2}$	-0.016	0.033

calcites

r = 0.19	*ilr1*	*ilr2*
$ilr1 = \frac{1}{\sqrt{2}} \cdot ln \frac{Ca}{Fe}$	0.050	0.033
$ilr2 = \frac{1}{\sqrt{6}} \cdot ln \frac{Ca \cdot Fe}{Mg^2}$	0.033	0.602

r = -0.83	*ilr1*	*ilr2*
$ilr1 = \frac{1}{\sqrt{2}} \cdot ln \frac{Fe}{Mg}$	0.436	-0.255
$ilr2 = \frac{1}{\sqrt{6}} \cdot ln \frac{Fe \cdot Mg}{Ca^2}$	-0.255	0.216

r = -0.79	*ilr1*	*ilr2*
$ilr1 = \frac{1}{\sqrt{2}} \cdot ln \frac{Ca}{Mg}$	0.492	-0.223
$ilr2 = \frac{1}{\sqrt{6}} \cdot ln \frac{Ca \cdot Mg}{Fe^2}$	-0.223	0.160

Table 2. Variance-covariance matrix and Pearson correlation index *r*, for *ilrs* balances in the 3 new spaces obtained; the matrices were calculated for each couple of balances and each group of minerals (calcites and ankerites).

In the three new plots (Figures 5-6-7), the possibility of modeling Ca/Fe/Mg ratios with linear regression (least squares method) between *ilrs* balances was evaluated.

For understanding some features of the joint distribution of data in the three diagrams, Mardia's test (e.g. Kankainen et al., 2004) on departure from bivariate normality for the two balances in each

system, on calcite and ankerites samples, has been preliminarily performed. Considering globally all the analyses divided by mineral (calcite and ankerite), both of carbonates not behave as normally distributed with respect to *ilrs* balances (hypothesis of bivariate normality refused, $p < 0.05$). Nevertheless, dividing the data on the base of depths in meter of drill core, the assumption of bivariate normality could be taken for ankerites subsets of data except for the level 3,868. The same operation of dividing in subsets calcites data resulted in a negative response for the level 3,865. For all the other ones the hypothesis of a normally joint distribution can be accepted.

Hereinafter in subsections 3.2.1 to 3.2.3, the graphics were commented; we commonly referred at "first balance" as the *ilr1* and "second balance" as the *ilr2*.

3.2.1

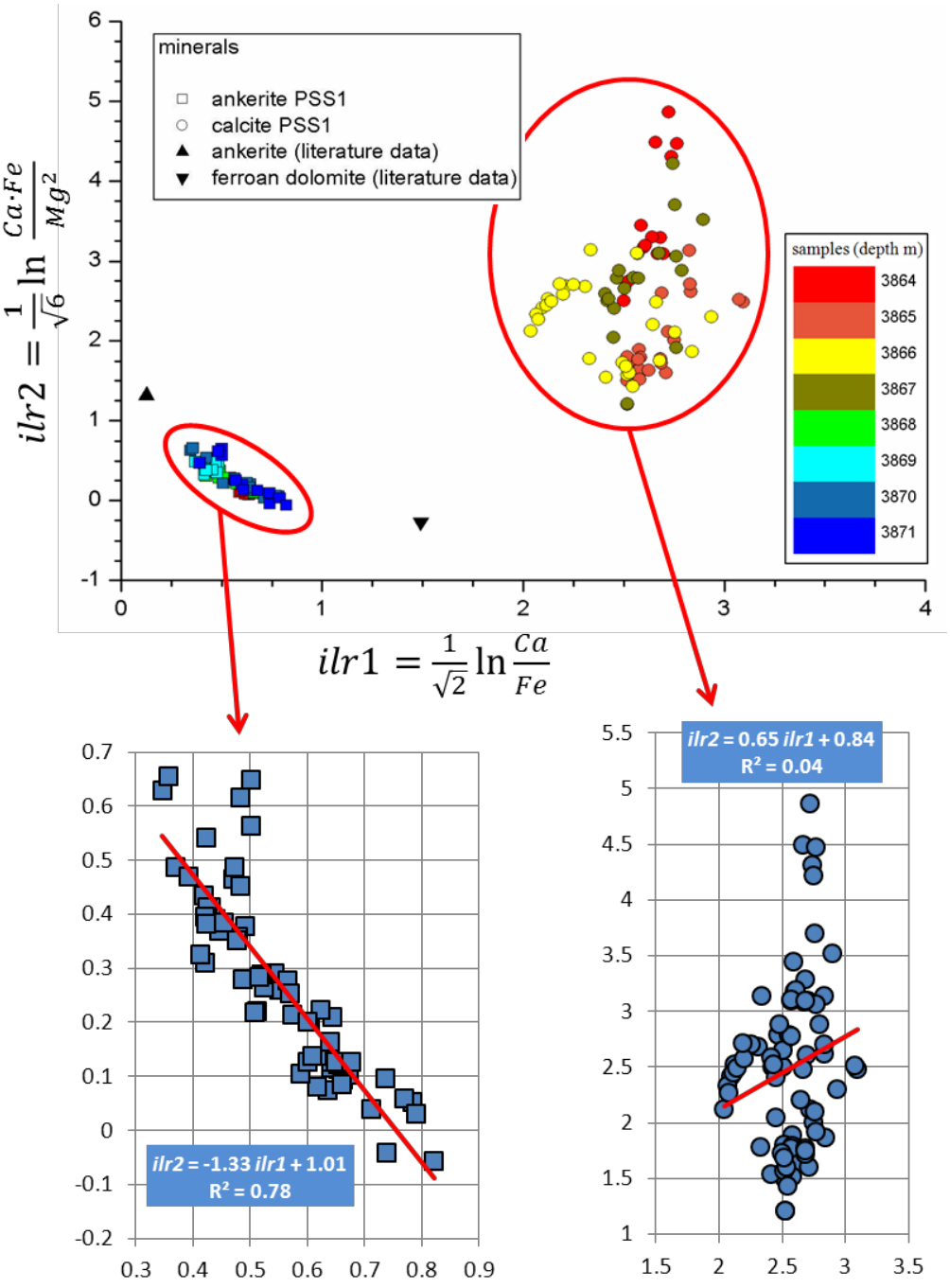

Figure 5. Binary diagram of *ilrs* balances; both ankerite and calcite minerals are shown in the upper diagram; symbol filling colours correspond to the depth (in m) at which the carbonates are found in the PSS1 drill cores. The lower diagrams represent, from left to right, tentative linear regression (red lines) modeling for ankerites and calcites, respectively. Equations of the regressions are reported, with least square R^2 values.

Ankerites

First balance showed variance value lower (0.013) than the second one (0.030); it means that when considering also magnesium other than calcium and iron the system become more variable.

Data pattern was modeled with a linear regression (R^2=0.78); removing samples from level 3,868 (for which the hypothesis of bivariate normality was refused) affected poorly the goodness of regression (R^2=0.79).

In any case slope values (varying from -1.33 to -1.32) of the linear regression told us that moving towards the left of the diagram (Ca/Fe ratio decreasing) the products (Ca·Fe) increase more than Mg^2.

Pearson correlation index value (-0.88) was high and negative and pointed out, as the regression, to an inverse relation between balances.

Calcites

Variance of first balance was high (0.050) compared to the one of ankerites, but one order of magnitude lower than the value of the *ilr2* (0.602); it means that calcium, iron and magnesium together are mutually related. Magnesium played a key role, as its introduction in *ilr2* increased dramatically variance.

Linear modeling resulted meaningless, also removing the level 3,865 (which contributed to refuse the hypothesis of bivariate normality as level 3,868 for ankerites) with R^2=0.04.

Pearson correlation index value (0.19) was low and positive, highlighting a poor positive correlation for the global dataset.

3.2.2

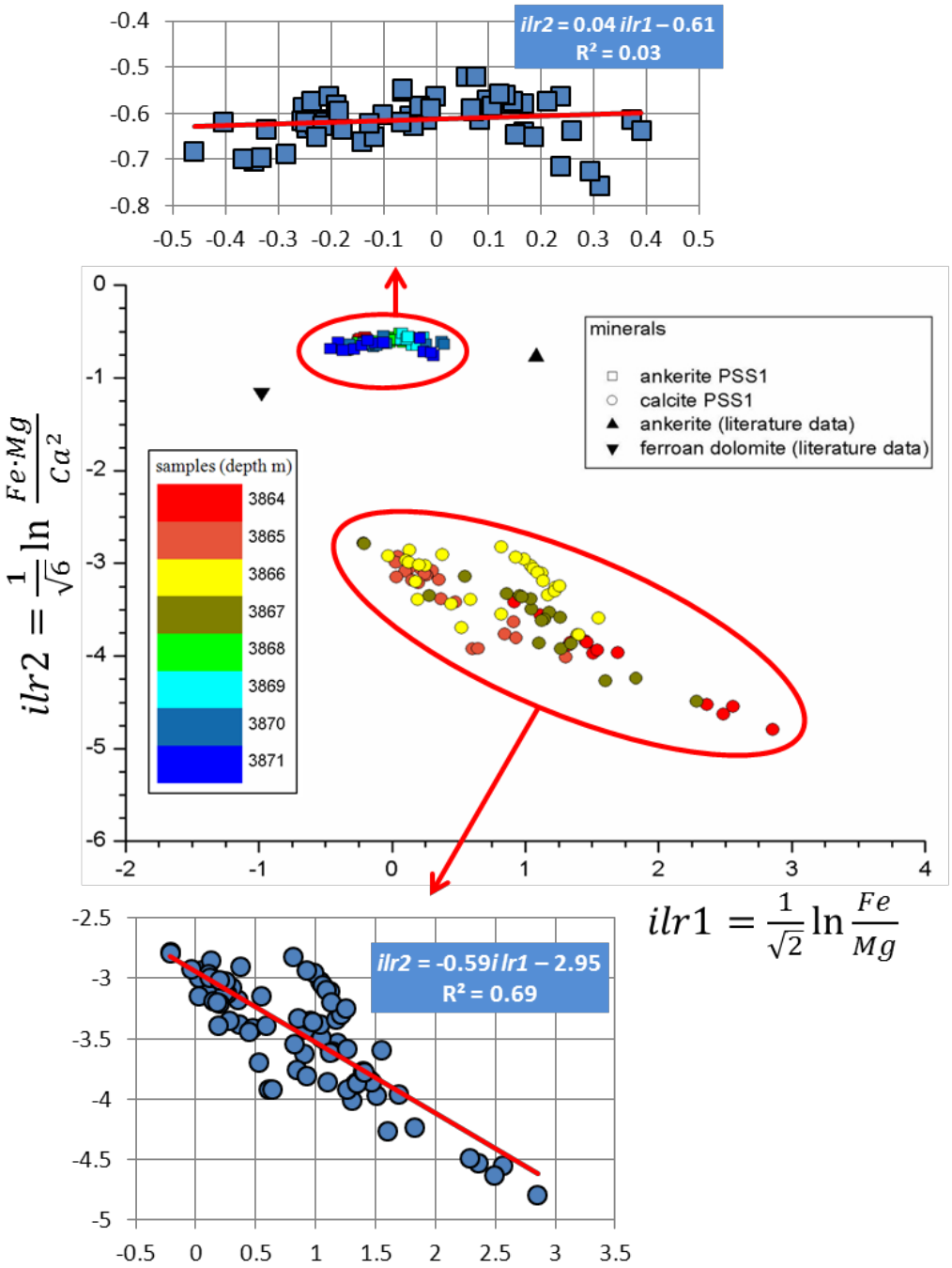

Figure 6. Binary diagram of *ilrs* balances; in the mid part are showed both carbonates minerals; symbol filling colours correspond to the depth (in m) at which the carbonates are found in the PSS1 drill cores. The two graphics upper and lower represent respectively ankerites and calcites tentative linear regression (red straights) modeling. Equations of the regressions are reported, with least square R^2 values.

Ankerites

First balance had variance value higher of more than an order of magnitude (0.041) with respect to the second one (0.002), which value was the lowest of all the balances for all the minerals. Ratio between Fe/Mg, centred nearly at 1 (0 in the *ilr1* axis), practically containing all the variability of the data structure of ankerites in that perspective; the introduction of Ca in the second balance seemed to have the only effects of normalize the variability expressed by the Fe/Mg ratio.

Modeling with regression the relation between balances was meaningless (R^2=0.03), Pearson correlation index value being (0.16) low and positive, highlighting a very poor positive correlation for the global dataset.

Calcites

The *ilr1* had variance value higher (0.436) than the second one (0.216), although the order of magnitude are the same instead of ankerite.

Linear modeling (R^2=0.69) showed little improvement in significance removing only level 3,865 (R^2=0.74), whereas excluding both 3,865 and 3,866 resulted in a dramatically increase of regression accuracy (R^2= 0.93).

In any case, slope values (respectively from -0.59 to -0.64 and -0.69) of the linear regression, told us that moving to the left of the diagram (Fe/Mg ratio decreasing), the products of (Fe·Mg) increase with respect to Ca^2.

Pearson correlation index value (-0.83) was high and negative, confirming that the two balances were inversely correlated.

3.2.3

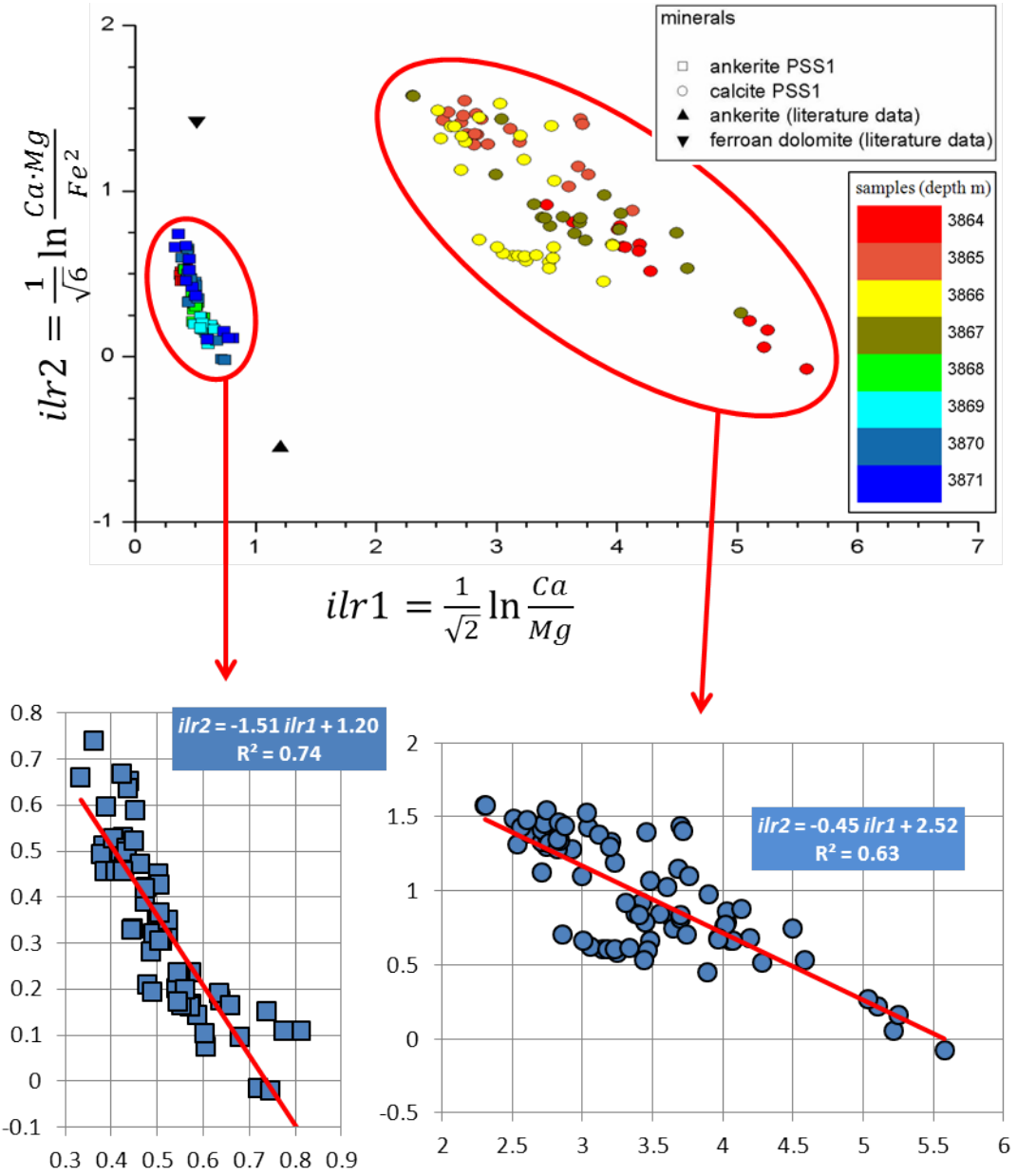

Figure 7. Binary diagram of *ilrs* balances; in the upper part are showed both carbonates minerals; symbol filling colours correspond to the depth (in m) at which the carbonates are found in the PSS1 drill cores. The two graphics lower represent respectively, from left to right, ankerites and calcites tentative linear regression (red straights) modeling. Equations of the regressions are reported, with least square R^2 values.

Ankerites

First balance showed variance value (0.011) lower than the second one (0.033). Considering also iron (*ilr2*), other than calcium and magnesium the variability of data tended to increase.

Data structure was modeled with regression (R^2=0.74), which significance improved a little by removing level 3,868 (R^2=0.76) or level 3,871 (R^2=0.80).

In any case, slope values (respectively from -1.51 to -1.54 and in the last case to -1.71) of the linear regression, told us that moving to the left of the diagram (Ca/Mg ratio decreasing) the products of (Ca·Mg) tend to increase with Fe^2.

Similarly to the diagram in Figure 5, Pearson correlation index value (-0.86) pointed out to an inverse correlation as indicated from regression analysis.

Calcites

The first coordinate *ilr1* had variance values higher (0.492) than the second one (0.160), on the contrary of ankerites.

Modeling was performed with linear regression (R^2=0.63); the exclusion of the level 3,866 (R^2=0.64) not affected the result whereas removing from dataset both 3,865 and 3,866 together improved significance of regression (R^2=0.90).

Slope values of the linear regression (respectively -0.45, -0.42 and -0.46), which are roughly 4 times smaller than the ones retrieved for ankerites, indicated the same trend described above for the latters. In this case, when Ca/Mg ratio decrease, (Ca·Mg) increases with the increase of Fe^2 even if slower than for ankerites.

Pearson correlation index value (-0.79) indicated a good inverse correlation for the whole data, according to the regression analysis.

4. Discussion

The binary diagrams of Figure 5 to Figure 7, obtained through *ilr* transformation of original data, suggested that for ankerites the variance of data set has to be mainly ascribed to substitutions between Fe and Mg. The majority of variance is expressed by the *ilr1* balance with Fe/Mg ratio (Figure 6), whereas in the *ilr2* balance, where Ca is included, the result is to normalize the (Fe·Mg) product, instead of adding variability to the data. Consequently, correlation and linear regression between the two balances mentioned above where not found in the dataset. This also indicates how Ca abundances are weakly dependent or nearly independent with respect to the Fe/Mg ratio. By comparing the slope values of regression in Figure 5 and Figure 7, we can assume that substitutions between Ca and Fe are slightly preferred to substitutions between Ca and Mg, being nevertheless strongly subordinated to Fe by Mg and Mg by Fe substitutions. These results are in agreement with those by Reeder and Dollase (1989) who highlighted that the first site for cations of ankerite is almost completely occupied (> 95%) by Ca, with a very small amount of Fe possibly substituting Ca, whilst the second site is filled by Mg and Fe with a wide range of Fe/Mg ratio values. Overall, the compositional data analysis has provided an interpretation that closely matches the structural features of ankerite.

Conversely, the processes that were able to explain the most variance of the dataset for calcites are substitutions between Ca and Mg and Fe and Mg. The values of Pearson correlation index between balances in diagrams where *ilr1* includes Ca/Mg and Fe/Mg are indeed both high and negative, with significant R^2 values (respectively 0.63 and 0.69) that tends to drastically increase when the data related to depths of 3,865 and 3,866 m are removed ($R^2 \geq 0.90$). Moreover, all the first coordinates *ilr1* with Mg have high values of variances. Variance value increases of one order of magnitude when the *ilr1* coordinate containing the Ca/Fe ratio is also considered, with respect to the corresponding *ilr2* that includes Mg, this cation clearly generating data variability. In the latter case, Mg behaves oppositely to what observed in the diagram for ankerites (Figure 6) where the effect of Ca is to normalize the product of the other two cations. For calcites, Mg heavily controls the pattern of the data, resulting in an increasing variability. Setting aside few samples at the depth of 3,867 m, the Fe/Mg ratio is always > 1, being Fe the second constituent of calcites. This can be explained by the fact that high-Mg calcites are unstable and tend to be substituted by high-Fe calcites, which are more thermodynamically stable (e.g. Richter and Füchtbauter, 1978).

Summarizing, the ankerite data structure of the PSS1 drill cores appears to be dominated by substitutions between Fe and Mg independently by Ca contents, whereas that of calcite is affected by Ca-Mg and Fe-Mg substitution pairs and practically involving all the sub-compositions considered, i.e. Ca-Fe-Mg.

Results also evidence that the variance of each *ilr* balance in the three systems is higher for calcite when compared to that for ankerite. The analysis of variance through *ilr* balances indicates that calcite composition is relatively more variable with respect to that of ankerite.

Moreover, in regression modeling the exclusion of 3,868 and 3,865 m deep "anomalous" layers, (which contribute to refuse the statistical hypothesis of bivariate normality) for ankerite and calcite, respectively provides better result for the latter, whereas ankerite is not affecting the significance of regression. The next step will be that to constrain and understand the how the substitution processes, for calcite and ankerite, have acted in the studied portion of the PSS1 well. In our opinion, this can be achieved by reconstructing the hypothetical mineral end-members for quantitative regression or mixture analysis. Literature data from http://webmineral.com/data have provided ankerite and ferroan dolomite compositions (reported in Figures 4 to 7) to be used as end-members externally to our compositional data. Some problems may be encountered for calcite, as the examples from literature data with not specified concentrations of iron or magnesium are unsuitable for plotting in the subcomposition, jeopardizing so far their use as potential end-members. Ferroan and magnesian calcites would be taken in account as possible candidates.

Local effects, evident in particular and affecting calcites composition in some levels (3,865 and 3,866), may be related a possible inhomogeneous sampling of drill-core from PSS1 bore-well. In this situation is recommended, in our opinion, to state only global considerations on the entire dataset and not for each one of the different levels of the drill-core.

5. Conclusions

Statistical (graphical and numerical) methods applied to mineral chemistry data of calcite and ankerite in drill cores from a high pCO_2 natural system in central-northern Italy after *ilr* transformation, as well as the right choice of the unit (atomic content %) for the abundance of the considered elements, allowed us to improve the understanding of relationships and processes affecting the dataset. Tools for compositional data analysis were employed by comparing the Ca, Fe and Mg concentrations of the two minerals in the same subcomposition.

The main result of this approach is that the behaviour of processes controlling stoichiometric substitutions of Ca-Fe-Mg in the ankerites structural sites is in agreement with what described in literature; high pCO_2 does not apparently have produced direct effects on substitutions processes. Differences with respect to calcites in substitutions processes could be related to either different structure (one site for divalent cations in calcite versus two sites in ankerite) or formation of calcites in different times and/or conditions, thus likely related to different steps in the fluid-rock interaction path that leaded to the observed paragenesis.

By combining the information obtained in this study and those from fluid inclusions, mineral chemistry, bulk rock analysis and numerical simulations of fluid-rock interactions, a better understanding on the role that CO_2 has played in determining the present mineral paragenesis and the fluid and rock composition in this natural high pCO_2 natural analogue can be achieved and possibly applied to CCS system.

Acknowledgments

This work was partially financed by a Project of Ciudad de la Energia (Spain) (Resp. for the CNR-IGG: O. Vaselli) and by PRIN (Italian Research Project of National Interest) 2007, prot. 2007M4K94A_002 (assigned to A. Buccianti).

References

Aitchison, J. (1986). *The Statistical Analysis of Compositional Data*. Monographs on Statistics and Applied Probability. Chapman & Hall Ltd., London (UK). (Reprinted in 2003 with additional material by The Blackburn Press). 416 p.

Anelli, L., Gorza, M., Pieri, M., and Riva, M. (1994). *Subsurface well data in the Northern Apennines (Italy)*. Memorie Società Geologica Italiana, 48, 461-471.

Bonini, M. (2009). *Structural controls on a carbon dioxide-driven mud volcano field in the Northern Apennines (Pieve Santo Stefano, Italy): Relations with pre-existing steep discontinuities and seismicity*. Journal of Structural Geology, 31, 44-54.

Buccianti, A., Mateu-Figueras, G., Pawlowsky-Glahn, V., editors (2006). *Compositional Data Analysis in the Geosciences from Theory to Practice*. Geological Society, Special Publication 264, London (UK). 224 p.

Egozcue, J. J., Pawlowsky-Glahn, V., Mateu-Figueras, G. and Barceló-Vidal, C. (2003). *Isometric logratio transformations for compositional data analysis*. Mathematical Geology, 35, 279-300.

E.N.I. (1984). *Pozzo Pieve Santo Stefano 1, Studio Petrografico delle vulcaniti e del loro inquadramento nell'ambito del vulcanesimo Oligo-miocenico nell'area del Mediterraneo Occidentale*. San Donato Milanese. 20 p.

Giggenbach, W. F., (1996). *Chemical composition of volcanic gases*. In: Monitoring and Mitigation of Volcanic Hazards. R. Scarpa & R.I. Tilling editors, Springer Verlag, Berlin-Heidelberg, Germany, 221-254.

Grunsky, E.C., Kjarsgaard, B.A., Egozcue, J.J., Pawlowsky-Glahn, V., Thió i Fernández de Henestrosa, S. (2008). *Studies in Stoichiometry with Compositional Data*. In: Proceedings of CODAWORK'08. 7 p.

Heinicke, J., Braun, T., Burgassi, P., Italiano, F., Martinelli, G. (2006). *Gas flow anomalies in seismogenic zones in the Upper Tiber Valley, Central Italy*. Geophysical Journal International, 167, 794–806.

Kankainen, A., Taskinen, S. and Oja, H. (2004). *On Mardia's tests of multinormality*. In: M. Hubert, G. Pison, A. Stryuf and S. Van Aelst, editors. Statistics for Industry and Technology, Birkhauser, Basel, 153-164.

Le Bas M.J., Le Maitre R.W., Streckeisen A. and Zanettin B. (1986). *A chemical classification of volcanic rocks based on the total alkali silica diagram*. Journal of Petrology, 27, 745-750.

Martin-Fernández, J.A., Barceló-Vidal, C., Pawlowsky-Glahn, V., Kovacs, L.O., Kovacs, G.P. (2005). *Subcompositional Patterns in Cenozoic Volcanic Rocks of Hungary*. Mathematical Geology, 37, 729-752.

Montegrossi, G., Ruggieri, G., Bicocchi, G., Vaselli, O., Burgassi, P., Tassi, F., Jordi, B. and Del Villar, L. P. (2010). *Modeling of mineral alteration in a natural CO_2 reservoir*. Acta Mineralogica et Petrographica, Abstract Series IMA 2010, 59.

Reeder, R.J., editor (1983). *Carbonates: mineralogy and geochemistry*. Reviews in Mineralogy and Geochemistry, Volume 11. 367 p.

Reeder, R.J., and Dollase W. A. (1989). *Structural variation in the dolomite-ankerite solid-solution series: An X-ray, Mössbauer, and TEM study*. American Mineralogist, 74, 1159-1167.

Richter, D.K, and Füchtbauer, H. (1978). *Ferroan calcite replacement indicates former magnesian calcite skeletons*. Sedimentology, 25, 843-860.

Sani, F., Bonini, M., Piccardi, L., Vannucci, G., Delle Donne, D., Benvenuti, M., Moratti, G., Corti, G., Montanari, D., Sedda, L., Tanini, C. (2009). *Late Pliocene-Quaternary evolution of outermost hinterland basins of the Northern Apennines (Italy), and their relevance to active tectonics*. Tectonophysics, 476, 336–356.